Deactivation of barium oxide-based NO$_x$ storage and reduction catalyst by hydrothermal treatment

Ji Won Park, Se Min Park, Young San Yoo*, Hyun-Sik Han* and Gon Seo[†]

School of Applied Chemical Engineering and Center for Functional Nano Fine Chemicals,
Chonnam National University, Gwangju 500-757, Korea
*HeeSung Catalysts Corporation, 1251-6 Jungwang-Dong, Shihung, Gyeonggi 429-786, Korea

Abstract−The deactivation of a barium oxide-based NO$_x$ storage and reduction (NSR) catalyst with hydrothermal treatment was studied by treating it with 10 vol% water vapor diluted in nitrogen at 850 °C. XRD, XPS, SEM, IR of CO adsorption, and the N$_2$ adsorption was used to investigate the physical and chemical changes of the NSR catalyst caused by the hydrothermal treatment. The 12 h hydrothermal treatment decreased its NO$_2$ storage capacity by 20%. However, the hydrothermal treatment significantly decreased its ability to reduce the stored NO$_2$. The formation of an inactive phase consisting of platinum and aluminum is believed to be the cause of the severe deactivation of the NSR catalyst.

Key words: NO$_x$ Storage and Reduction (NSR), Barium Oxide, Deactivation, Hydrothermal Treatment

INTRODUCTION

The reduction of harmful materials from automobile exhaust is believed to be the most urgent task for clean air because automobiles account for 85% of air pollutants released into the atmosphere [1]. Pollutants from gasoline engines such as unburned hydrocarbons (HC), carbon monoxide (CO), and nitrogen oxides (NO$_x$) are removed simultaneously over three-way catalysts through balanced oxidation-reduction reactions [2]. However, three-way catalysts cannot be applied to diesel engine exhaust because they are operated with excess oxygen to enhance the fuel combustion efficiency. Since excess oxygen in exhaust gasses suppresses the reduction reaction of NO$_x$, other methods are needed to remove NO$_x$ from diesel exhaust.

A selective catalytic reduction (SCR) system using urea as a reductant is quite effective in removing NO$_x$ from diesel engines because urea works as an active reductant like ammonia [3,4]. However, the requirement of additional equipment for the storage and injection of urea is an impediment to its commercial application to automobiles.

The NO$_x$ storage and reduction (NSR) catalytic system is quite convenient compared with the SCR system [5,6]. There is no need for additional equipment because fuel is used as the reductant. NO$_x$ is stored on barium oxide at oxidative periods. The injection of fuel pulses periodically converts the reaction atmosphere to a reductive one, which allows the stored NO$_x$ to be desorbed and reduced to nitrogen by fuel over noble metals. Noble metals also oxidize nitrogen monoxide (NO) to nitrogen dioxide (NO$_2$) for the stable storage of NO$_x$. The allowed limit of NO$_x$ removal can be achieved on NSR catalysts by enhancing their NO$_x$ storage capacity and adjusting the injection size and interval of the fuel pulses [7,8].

Although NSR catalysts usually show a high performance for the removal of NO$_x$ from diesel engines at their fresh state, their activity decreases considerably when working as deNO$_x$ catalysts. Sulfur dioxide (SO$_2$) produced from sulfur compounds in fuel poisons irreversibly the loaded noble metals. SO$_2$ molecules also react with the storage materials in the NSR catalysts, thereby reducing their NO$_x$ storage capacity [9-11]. The other cause for deactivation is hydrothermal aging because NSR catalysts are inevitably exposed to water vapor at elevated temperatures. The hydrothermal treatment of metals and metal oxides over a long period induces physical and chemical changes [12-14].

However, there have not been any extensive studies on the deactivation of NSR catalysts by hydrothermal treatment compared with that by SO$_2$ [15,16]. We examined the hydrothermal deactivation of an NSR catalyst provided by HeeSung Catalysts Corporation. Barium oxide was supported on γ-alumina as a NO$_x$ storage material. Noble metals catalyze the oxidation of NO to NO$_2$ as well as the reduction of the desorbed NO$_2$. The NO$_2$ storage capacity and the reduction activity of the stored NO$_2$ of the catalyst were examined after treating it with water vapor diluted in nitrogen. The changes in the physical and chemical properties of the catalyst in terms of its catalytic performance were investigated in order to determine the cause of the hydrothermal deactivation.

EXPERIMENTAL

An NSR catalyst provided by HeeSung Catalysts Corporation was used in this deactivation study. Barium oxide was impregnated on γ-alumina (SASOL, surface area 150 m^2/g) as an NO$_2$ storage material. Platinum and rhodium were also impregnated for the oxidation of NO under lean conditions and for the reduction of desorbed NO$_2$ under rich conditions. The chemical composition of the catalyst was determined to be BaO (5.6 wt%) and Pt (0.7 wt%) by using an energy dispersive x-ray spectroscope (EDX, NORAN Z-MAX 300 Series) attached to a scanning electron microscope (SEM, JEOL JSN-5400).

[†]To whom correspondence should be addressed.
E-mail: gseo@chonnam.ac.kr

The catalyst was treated in a nitrogen flow of 100 ml/min containing 10 vol% water vapor at 850 °C. The treatment time was varied from 4 to 12 h. The NSR catalysts were classified as either fresh and aged catalysts, and denoted as NSR (fresh), NSR (aged_4), NSR (aged_8), and NSR (aged_12) catalyst to indicate the treating time.

The X-ray diffraction (XRD) patterns of the catalysts were recorded on an X-ray diffractometer (Rigaku D/Max Ultima III) with Cu Kα X-ray at 40 kV and 40 mA. The N_2 adsorption isotherms of the catalysts were obtained at liquid nitrogen temperature by using an automatic volumetric adsorption system (Mirae SI nanoPorosity-XG). The catalysts were evacuated at 200 °C for 1 h prior to the adsorption experiment. Their surface areas and average pore diameters were calculated by using the BET equation and BJH method, respectively.

The surface composition and oxidation state of the active ingredients of the fresh and aged NSR catalysts were examined by X-ray photoelectron spectroscopy (XPS, VG MultiLab 2000) with a Mg Kα X-ray source of 300 W. The binding energy of the C1s peak was set to 285.0 eV and used as a reference. The catalysts were sputtered by an Ar^+ beam for 180 s to determine their internal composition. The sputtering rate of the Ar^+ beam was 1-2 Å/s for a SiO_2 film.

The CO adsorbed on the catalysts was determined by using a Fourier-transformed infrared spectrophotometer (FT-IR, Bio-Rad, FTS-175C). A self-supported catalyst wafer was charged in an *in-situ* cell (Graseby Specac) and evacuated at 500 °C for 1 h. The evacuated catalyst wafer was exposed to CO (Donga, 99.6%) of 50 Torr at 50 °C for 20 min. Before recording the IR spectra, the cell was evacuated to remove the gaseous CO.

The IR spectra of NO_2 stored on the catalyst were recorded by the same procedure for those of adsorbed CO. Evacuated catalyst wafers were exposed to NO_2 gas (Donga, 99.5%) at a pressure of 5 Torr at 200 °C and evacuated to remove the gaseous NO_2. After the spectra were recorded, hydrogen gas (Sinil, 99.9%) at a pressure of 15 Torr was introduced to the cell to reduce the stored NO_2. The IR spectra of the catalysts recorded after evacuation revealed their regenerated states.

The amount of NO_2 stored on the catalysts was measured with a gravimetric adsorption system equipped with a quartz spring balance [17]. The catalysts were evacuated at 300 °C for 1 h and exposed to NO_2 gas at a pressure of 10 Torr at 200 °C. The amount of NO_2 stored on the catalysts was determined from the increase in mass after exposure to NO_2 followed by evacuation.

The desorption of NO_2 from the catalysts was investigated by using a home-made temperature programmed desorption (TPD) system. A catalyst sample of 0.1 g was activated in a nitrogen gas flow of 100 ml/min at 550 °C for 1 h. The catalyst was saturated with NO_2 at 200 °C by injecting NO_2 pulses followed by nitrogen purges to remove the weakly and physically adsorbed NO_2. The desorbed NO_2 was monitored with an NO_2 analyzer (NGK TNS-1111-20A) with increasing temperature at 10 °C/min.

The storage and reduction performance of the NSR (fresh) and NSR (aged_12) catalysts of a honeycomb-shaped monolith was evaluated on an engine dynamometer operated under repeated lean and rich cycles. A gasoline-powered engine with 3.5 L of engine displacement was used to exclude the effect of particulate matter on the deNO$_x$ activity of NSR catalysts. The concentration of input

NO$_x$ was adjusted to 1,500 ppm to obtain the performance at an extraordinary severe condition. Lambda values were 1.2 and 0.95 at lean and rich cycles, respectively. The volume of the catalyst bed was 0.75 L and the space velocity was adjusted to 54,000 h^{-1} at 300 °C. The test run was begun with fuel injection to maintain the fuel rich condition. After the duration of the fuel rich condition for 120 s, the atmosphere of the exhaust gas was converted to a fuel lean condition by stopping the fuel injection. The fuel lean and rich conditions were repeated at 60 s and 2 s intervals, respectively. The test run was composed of ten repeated operations and ended at the fuel rich condition. The performance of the NSR catalysts was measured at 200 °C, 300 °C and 400 °C to determine their temperature dependence. The NO$_x$ reduction activity of the catalysts was defined as the percentage of NO$_x$ reduced of the total amount of NO$_x$ in the exhaust gas measured by using an NO$_x$ analyzing system coupled with a dynamometer.

RESULTS AND DISCUSSION

1. Deactivation of the NSR Catalyst

The barium oxide-based NSR catalyst was considerably deactivated after the hydrothermal treatment. Fig. 1 shows the performance of the NSR (fresh) and NSR (aged_12) catalysts in the test run of the engine dynamometer at 300 °C. At the starting fuel rich condition, the reduction activity of NO$_x$ on the NSR (fresh) catalyst was almost complete. After the fuel injection was stopped, the reduction activity of NO$_x$ decreased rapidly due to the depletion of the reductants. However, the atmosphere of the exhaust gas was changed again to a reductive atmosphere by injecting a fuel pulse. The amount of desorbed NO$_x$ was reduced, resulting in a sharp increase in the NO$_x$ reduction activity. The NO$_x$ reduction activity decreased rapidly after stopping of the fuel injection, but increased sharply again with the fuel injection due to the increased concentration of reduc-
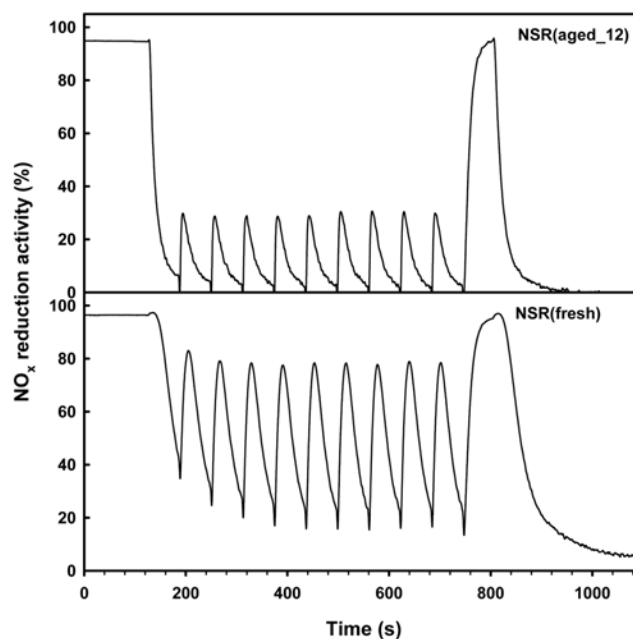

Fig. 1. NO$_x$ reduction over the NSR (fresh) and NSR (aged_12) catalysts in the test run of an engine dynamometer at 300 °C.

tants in the exhaust.

The appropriate time interval of the fuel injection is important for maintaining the deNO$_x$ activity. The peak values of the NO$_x$ reduction activity were approximately 80% on the NSR (fresh) catalyst, which indicates good performance. Furthermore, there was no substantial decrease in activity with time. However, the aged NSR catalysts showed much lower activity than the fresh one. The peak values of the NO$_x$ reduction activity on the NSR (aged_12) catalyst were approximately 30%. The 12 h hydrothermal treatment of the NSR catalyst caused severe deterioration in the performance of the NO$_x$ reduction.

The performance of the NSR catalyst is strongly dependent on the reaction temperature, as shown in Fig. 2. The NO$_x$ reduction activity was highest at 300 °C both over the NSR (fresh) and NSR (aged_12) catalysts in the range of 200 °C and 400 °C. Too much adsorption of NO$_2$ on the NSR catalyst at low temperatures and too

little adsorption at high temperature may result in maximum performance at an intermediate reaction temperature. The activities of the aged catalysts were much lower at this temperature range compared with the fresh one. Since there are no contaminants such as sulfur and arsenic in the test fuel, the deactivation of the NSR catalyst must be the result of the hydrothermal treatment causing changes in the physical structure and chemical state of its active ingredients.

2. The Physical Structure of the NSR Catalyst

Fig. 3 shows the XRD patterns of the fresh and aged NSR catalysts highlighting the changes in the structure of the active ingredients during the hydrothermal treatment. The characteristic diffraction peaks of ceria along with those of alumina were observed on the NSR (fresh) catalyst. Although barium oxide is the major component, there were no diffraction peaks for barium oxide on the XRD patterns. This means that most ingredients of the NSR catalyst were highly dispersed on alumina, while there was relatively poor dispersion of ceria.
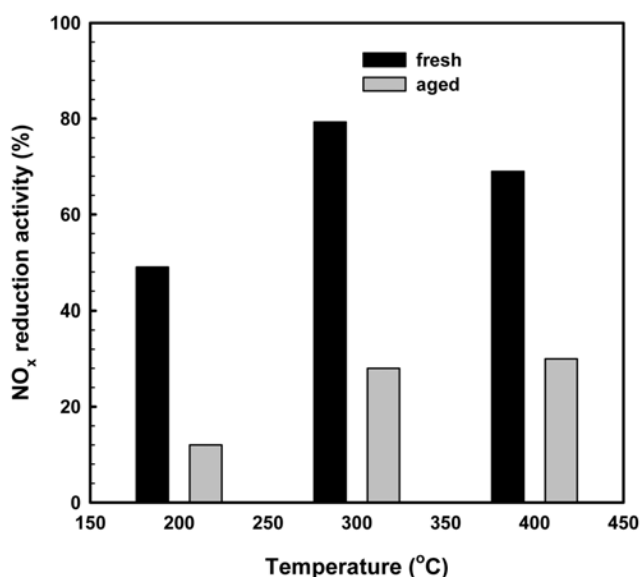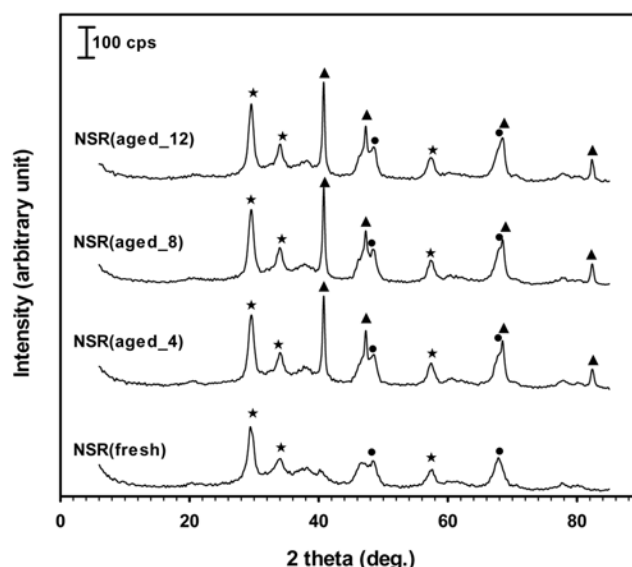

Fig. 2. Comparison the NO$_x$ reduction over the NSR (fresh) and NSR (aged_12) catalysts in the test run of an engine dynamometer at various temperatures.

Fig. 3. X-ray diffraction patterns of the fresh and aged NSR catalysts. ★; CeO$_2$, ▲; AlPt$_3$, ●; Al$_2$O$_3$.
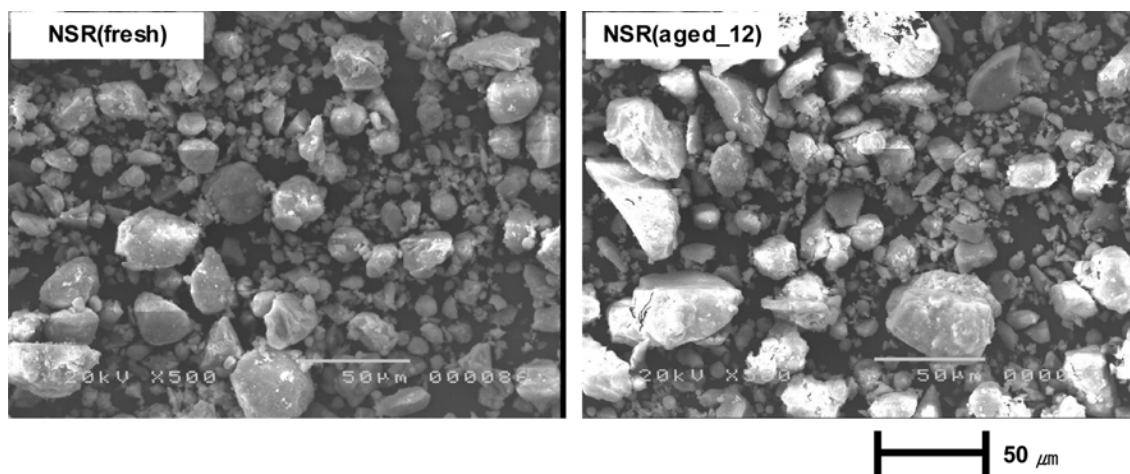

Fig. 4. SEM images of the NSR (fresh) and NSR (aged_12) catalysts.

The diffraction peaks attributed to alumina and ceria on the NSR catalyst increased slightly with the hydrothermal treatment, indicating a small increase in their crystallinity. A definite difference in the XRD patterns of the aged NSR catalysts compared with that of the fresh one was the appearance of characteristic peaks assigned to $AlPt_3$. The peaks observed at 40°, 48°, 69° and 83° confirmed the formation of $AlPt_3$ [18,19]. Some of the platinum atoms reacted with alumina and produced crystalline $AlPt_3$. The formation of $AlPt_3$ inevitably induces a loss of exposed platinum metal atoms, which work as active sites for the oxidation of NO to NO_2 as well as for the reduction of desorbed NO_2, resulting in severe deactivation of the NSR catalyst in the reduction of desorbed NO_2.

In contrast, there were no significant changes in the SEM images of the NSR catalyst with the hydrothermal treatment, as shown in Fig. 4. The large particles were slightly larger on the NSR (aged_12) catalyst, but small particles still remained even after the hydrothermal treatment for 12 h.

There was also no remarkable change in the nitrogen adsorption-desorption isotherms of the NSR catalyst with the hydrothermal treatment, as shown in Fig. 5. The shapes of the isotherms and the sizes of the hysteresis loops were almost the same in both the NSR (fresh) and NSR (aged_12) catalysts. Table 1 shows the surface areas and mesopore volumes of the NSR catalysts determined from their
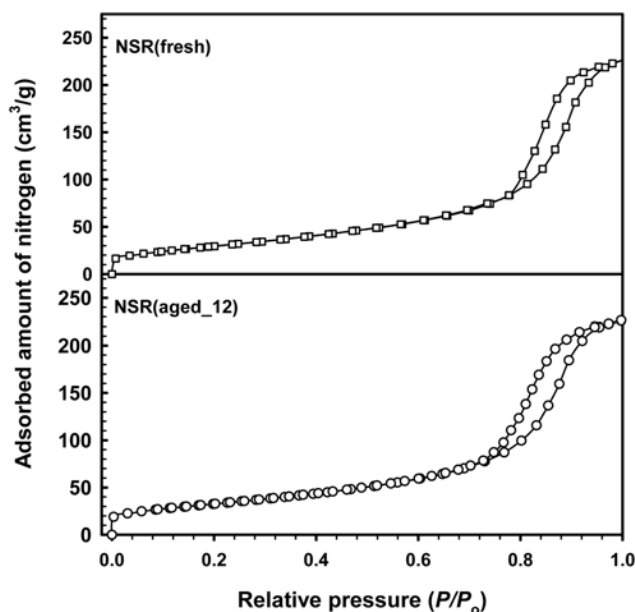
nitrogen adsorption-desorption isotherms. The negligible difference in surface area and mesopore volume with the hydrothermal treatment indicates that there was no significant sintering and migration of alumina support.

An examination of the surface composition and oxidation state of noble metals loaded on the NSR catalyst from their XPS spectra was very difficult because their loading levels were quite small. The major component of the catalyst surface was aluminum. The atomic % barium was approximately 2-3%, but that of platinum was less than 0.2%. The hydrothermal treatment did not induce any remarkable change in the XPS peaks of aluminum and barium. However, it was impossible to confirm the change in the chemical state of the noble metals after the hydrothermal treatment because of their extremely small peaks.

On the other hand, the adsorption property of CO on the NSR catalyst definitely changed as a result of the hydrothermal treatment. As shown in Fig. 6, the adsorption of CO on the NSR (fresh) catalyst caused the appearance of several absorption bands. The band at 2,065 cm^{-1} was assigned to CO adsorbed on platinum metal atoms, and the bands at 1,354 and 1,600 cm^{-1} were assigned to barium carbonate [20]. However, the band at 2,065 cm^{-1} did not appear on the aged NSR catalysts even when they were exposed to CO. The bands attributed to barium carbonate were similarly observed while they became broad. The disappearance of the 2,065 cm^{-1} band on the aged NSR catalysts indicates a significant loss of exposed platinum metal atoms during the hydrothermal treatment, but the retention of the 1,354 and 1,600 cm^{-1} bands shows the presence of barium oxide on their surface. A comparison of the amounts of CO adsorbed on the fresh and aged NSR catalysts was not made because they contained other ingredients that participate in CO adsorption
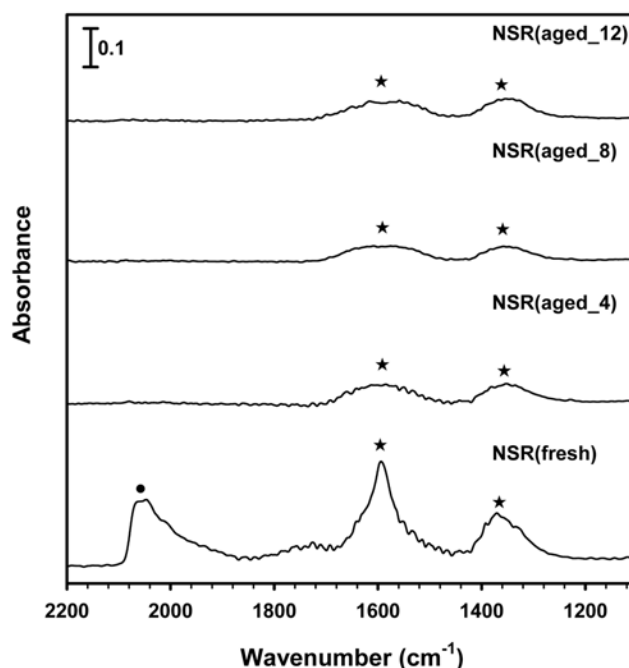

Fig. 5. N_2 adsorption isotherms of the NSR (fresh) and NSR (aged_12) catalysts.

Table 1. Surface areas and mesopore volumes of the fresh and aged NSR catalysts

	S_{BET} (m^2/g)	Mesopore volume (cm^3/g)	Average pore diameter (nm)
NSR (fresh)	118	0.35	10.5
NSR (aged_4)	114	0.36	10.7
NSR (aged_8)	105	0.35	12.3
NSR (aged_12)	108	0.35	11.0

Fig. 6. IR spectra of CO adsorbed on the fresh and aged NSR catalysts. The evacuated catalysts were exposed to CO of 50 Torr at 50 °C followed by evacuation. ★; barium carbonate, ●; Pt-CO.
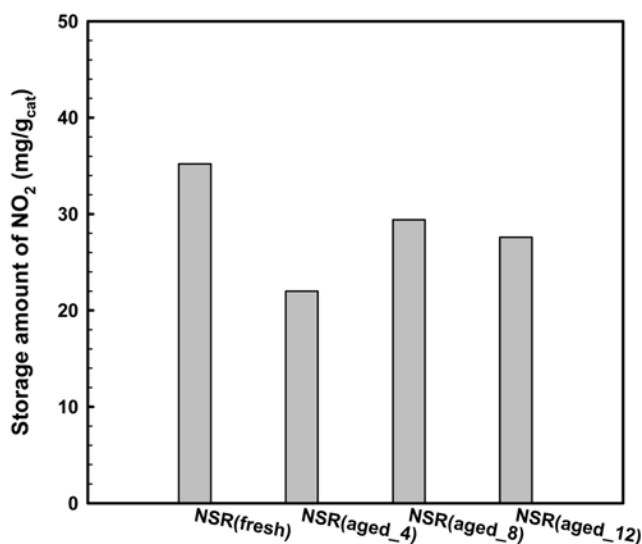
Fig. 7. The amounts of NO₂ stored on the fresh and aged NSR catalysts at 200 °C.

[21,22].

3. The Storage Capacity of the NSR Catalysts

The storage of NO_2 on barium oxide is sensitive to its surface structure. Fig. 7 shows the amounts of NO_2 stored on the fresh and aged NSR catalysts at 200 °C. Since the amounts of NO_2 stored denote the uptakes of NO_2 after evacuation, they represent the amounts of NO_2 captured on the catalysts. The amounts of NO_2 stored on the aged NSR catalysts were small compared with that on the NSR (fresh) catalyst, but the decrease in the storage capacity of the NSR catalyst due to the hydrothermal treatment was not significant. The small amount of NO_2 stored on the NSR (aged_4) catalyst compared to the aged NSR catalysts for longer periods shows the low consistency of the decrease in the storage capacity with the hydro-
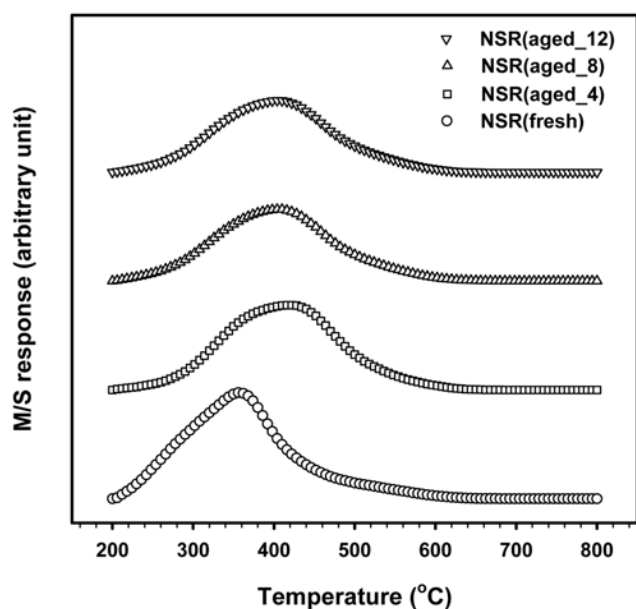

Fig. 8. TPD profiles of NO₂ from the fresh and aged NSR catalysts.
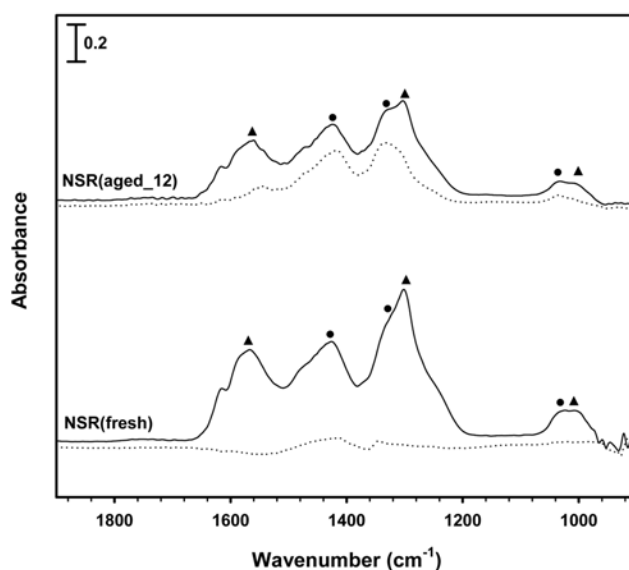

Fig. 9. IR spectra of NO₂ stored on the NSR (fresh) and NSR (aged_12) catalysts recorded after exposing the catalyst to NO₂ (solid) and regeneration by hydrogen (dot) at 200 °C. ▲; bidentate nitrate, ●; ionic nitrate.

thermal treatment.

The desorption profiles of NO_2 from the aged NSR catalysts were also similar to that from the fresh NSR catalyst, as shown in Fig. 8. The desorption peak of NO_2 from the NSR (fresh) catalyst was sharp but those from the aged NSR catalysts were broad. Although the peak shape of NO_2 desorbed changed after the hydrothermal treatment, the peak area was almost the same. The small difference in the peak areas of NO_2 desorption confirms that the storage capacity of NO_2 on the NSR catalysts remains at similar levels even after the hydrothermal treatment.

The activity of the NSR catalysts in NO_2 reduction decreased significantly with the hydrothermal treatment. Fig. 9 shows the IR spectra of NO_2 stored on the NSR (fresh) and NSR (aged_12) catalysts. The absorption bands of NO_2 could be assigned to ionic and bidentate nitrates [23,24]. The large bands of NO_2 on the fresh catalyst indicate its large storage capacity. The complete disappearance of NO_2 bands with the hydrogen treatment revealed its high reduction activity for stored NO_2. The decrease in the intensity of the NO_2 absorption bands on the NSR (aged_12) catalyst indicated a decrease in the storage capacity of NO_2 as a result of the hydrothermal treatment. More important was that the NO_2 bands that appeared on the aged NSR catalyst were not completely removed after the hydrogen treatment. Half of them remained even after exposure to hydrogen at a pressure of 15 Torr at 200 °C, indicating severe deterioration in the reduction activity of the NSR catalyst.

The performance of the NSR catalysts is strongly dependent on the storage capacity of NO_x at the oxidative condition and the reduction activity of the desorbed NO_2. The storage capacity of NO_2 on the NSR catalyst decreased as a result of the hydrothermal treatment, but the decrease was not large. However, the NO_x reduction activity of the NSR catalyst decreased significantly after the hydrothermal treatment. Therefore, the decrease in the performance of the NSR catalyst measured at the engine test was mainly caused

by the deactivation of noble metals, not by a reduction in the NO_x storage capacity.

The formation of an inactive phase of platinum $AlPt_3$ was responsible for the deactivation of the NSR catalyst. A loss of active platinum atoms reduces the activity for the stored NO_2. Although the deactivation of NSR catalysts with sulfur-containing species is due to both the significant reduction of the NO_x storage capacity and severe poisoning of noble metals, the hydrothermal treatment mainly decreases the reduction activity of the NSR catalyst due to the formation of an inactive phase of noble metals.

CONCLUSIONS

The hydrothermal treatment significantly deactivated the NSR catalyst prepared by impregnating barium oxide, noble metals and promoters. There was no significant decrease in the storage capacity of the NSR catalyst even after hydrothermal treatment for 12 h, but there was a severe loss of the NO_x reduction activity. Therefore, the disappearance of active platinum metal atoms due to the formation of $AlPt_3$ is believed to be responsible for the deactivation of the NSR catalyst.

ACKNOWLEDGMENTS

REFERENCES

1. F. Garin, *Appl. Catal. A: Gen.*, **222**, 183 (2001).
2. J. A. Botas, N. A. Gutierrez-Ortiz, M. P. Gonzalez-Marcos, J. A. Gonzalez-Marcos and J. R. Gonzalez-Velasco, *Appl. Catal. B: Environ.*, **35**, 243 (2001).
3. M. A. Larrubia, G. Ramis and G. Busca, *Appl. Catal. B: Environ.*, **27**, L145 (2000).
4. M. Koebel, M. Elsener and M. Kleemann, *Catal. Today*, **59**, 335 (2000).
5. N. Takahashi, H. Shinjoh, T. Iijima, T. Suzuki, K. Yamazaki, K. Yokota, H. Suzuki, N. Miyoshi, S. Matsumoto, T. Tanizawa, T. Tanaka, S. Tateishi and K. Kasahara, *Catal. Today*, **27**, 63 (1996).
6. Y. Su and M. D. Amiridis, *Catal. Today*, **96**, 31 (2004).
7. W. S. Epling, J. E. Parks, G. C. Campbell, A. Yezerets, N. W. Currier and L. E. Campbell, *Catal. Today*, **96**, 21 (2004).
8. S. Matsumoto, *Catal. Today*, **29**, 43 (1996).
9. S. Poulston and R. R. Rajaram, *Catal. Today*, **81**, 603 (2004).
10. Ch. Sedlmair, K. Seshan, A. Jentys and J. A. Lercher, *Catal. Today*, **75**, 413 (2002).
11. A. Amberntsson, E. Fridell and M. Skoglundh, *Appl. Catal. B: Environ.*, **46**, 429 (2003).
12. S. Elbouazzaoui, X. Courtois, P. Marecot and D. Duprez, *Top. Catal.*, **30-31**, 493 (2004).
13. B.-H. Jang, T.-H. Yeon, H.-S. Han, Y.-K. Park and J.-E. Yie, *Catal. Lett.*, **77**, 21 (2001).
14. K. Yamazaki, N. Takahashi, H. Shinjoh and M. Sugiura, *Appl. Catal. B: Environ.*, **53**, 1 (2004).
15. J. A. Anderson, Z. Liu and M. F. Garcia, *Catal. Today*, **113**, 25 (2006).
16. P. T. Fanson, M. R. Horton, W. N. Delgass and J. Lauterbach, *Appl. Catal. B: Environ.*, **46**, 393 (2003).
17. S. M. Park, J. W. Park, H.-P. Ha, H.-S. Han and G. Seo, *J. Mol. Catal. A. Chem.*, **273**, 64 (2007).
18. W. Bronger, K. Wrzesien and P. Muller, *Solid State Ion.*, **101-103**, 633 (1997).
19. PDF Card, PDF#29-0070.
20. X. Liu, O. Korotkikh and R. Farrauto, *Appl. Catal. A. Gen.*, **226**, 293 (2002).
21. J. J. Daniels, A. R. Arther, B. L. Lee and S. M. Stagg-Williams, *Catal. Lett.*, **103**, 169 (2005).
22. B. A. Riguetto, S. Damyanova, G. Gouliev, C. M. P. Marques, L. Petrov and J. M. C. Bueno, *J. Phys. Chem. B*, **108**, 5349 (2004).
23. F. Prinetton, G. Ghiotti, I. Nova, L. Lietti, E. Tronconi and P. Forzatti, *J. Phys. Chem. B*, **105**, 12732 (2001).
24. B. Westerberg and E. Fridell, *J. Mol. Catal. A. Chem.*, **165**, 249 (2001).